Electronic Supplementary Material (ESI) for Dalton Transactions.

Supporting Information for

Ring-Opening Polymerization of *rac*-Lactide and α-Methyltrimethylene Carbonate Catalyzed by Magnesium and Zinc Complexes Derived from Binaphthyl-based Iminophenolate Ligands

Miao Huang, Chen Pan and Haiyan Ma*

Shanghai Key Laboratory of Functional Materials Chemistry and Laboratory of Organometallic Chemistry, East China University of Science and Technology, 130 Meilong Road, Shanghai 200237, P. R. China.

* To whom correspondence should be addressed. Tel./Fax: +86 21 64253519. E-mail: haiyanma@ecust.edu.cn.

Contents:

Figure S13. A) ^{1}H NMR spectrum of *rac*-lactide oligomer obtained by complex **4a**/ ^{i}PrOH system; B) ^{1}H NMR spectrum of complex **4a**; C) ^{1}H NMR spectrum of free ligand $\mathbf{L^4H}$.

Figure S14. ^{1}H NMR spectrum of *rac*-lactide oligomer obtained by complex **4a**/^{i}PrOH system.

Figure S15. ^{1}H NMR spectrum of polymer sample obtained from the **4a**-isopropanol system.

Figure S16. ESI-TOF mass spectrum of the *rac*-LA oligomer obtained with **4a** ([*rac*-LA]$_0$: [**4a**]$_0$: [^{i}PrOH]$_0$ = 20:1:1, in THF).

Figure S17. Homonuclear decoupled ^{1}H NMR spectrum of PLA produced from *rac*-lactide using **4b** as initiator.

Figure S18. Details of the carbonyl region of the ^{13}C{^{1}H} NMR spectra of poly(α-MeTMC) obtained by **4a**, **5a**, **6a**, **4b.**

Figure S19. The DSC curves of poly(α-MeTMC) produced from α-MeTMC using **4b** as initiator.

.

Table S1. Chemical shifts of Ar-NMe_2 resonances in the ^{1}H NMR spectra of complexes **4a**-**6a**, **4b** and corresponding proligands [a]

	Ar-N(CH_3)$_2$			Ar- N(CH_3)$_2$
Complex	C_6D_6	C_6D_6 with THF [b]	Ligand	C_6D_6
4a	2.26 (s)	2.16 (s)	$\mathbf{L^4H}$	2.21
5a	2.25 (s)	2.20 (s)	$\mathbf{L^5H}$	2.20

6a	2.25 (s)	2.23 (s)	**L^6H**	2.22
4b	1.98 (s)	2.03 (s)	**L^4H**	2.21

[a]: In ppm, C_6D_6, 400 MHz, 25 °C; [b]: One tiny drop of THF was added to the solution of metal complex in C_6D_6.

Table S2. Crystallographic data for **4a, 4b** and **5b'**

	4a	**4b**	**5b'**
Empirical formula	$C_{53}H_{61}MgN_3OSi_2$	$C_{53}H_{61}N_3OSi_2Zn$	$C_{105}H_{86}N_4O_2Zn$
Formula weight	836.54	877.60	1501.15
Temp (K)	293(2)	293(2)	140(2)
Crystal size (mm)	0.213 x 0.147 x 0.123	0.267 x 0.211 x 0.147	0.16 x 0.12 x 0.10
Crystal system	Monoclinic	Triclinic	Triclinic

Space group	P2(1)/n	P-1	P-1
a (Å)	13.584(9)	9.1425(8)	14.188(2)
b (Å)	14.016(9)	14.6284(12)	14.372(2)
c (Å)	26.244(19)	18.6227(16)	24.466(5)
α (º)	90	83.526(2)	103.998(5)
β (º)	99.684(12)	88.281(2)	95.315(5)
γ (º)	90	87.762(2)	112.577(3)
Volume (Å^3)	4925(6)	2472.0(4)	4373.0(14)
Z	4	2	2
Density$_{cal}$ (mg/m^3)	1.128	1.179	1.140
Abs coeff (mm^{-1})	0.124	0.584	0.332
F (000)	1792	932	1580
θ range (º)	1.57 to 25.50	1.68 to 26.00	0.88 to 26.00
Data collected (*hkl*)	–9 to 16, –15 to 16, –28 to 31	±11, –18 to 13, ±22	±17, ±17, –24 to 30
Reflns collected/unique	26959 / 9012	15166 / 9707	31704 / 17112
R (int)	0.2455	0.0295	0.0748
Max. and min. transmn	1.00000 and 0.23415	1.00000 and 0.14173	0.9675 and 0.9488
Data/restrains/para	9012 / 0 / 554	9707 / 0 / 553	17112 / 618 / 1016
Goodness-of-fit on F^2	0.826	1.010	0.977
Final R_1,wR_2 [I > 2σ(I)]	0.0774, 0.1136	0.0530, 0.1352	0.0724, 0.1861
R_1, wR_2 (all data)	0.3055, 0.1785	0.0791, 0.1534	0.1262, 0.2214
$\Delta\rho_{max, min}$/e Å^{-3}	0.200 and –0.234	0.522 and –0.309	0.529 and –0.497

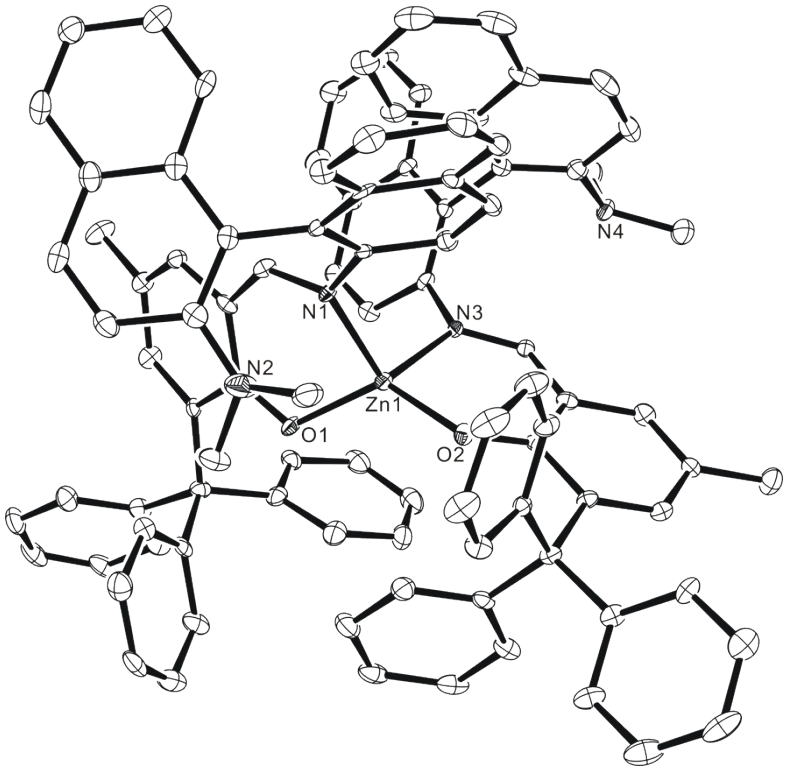

Figure S1. ORTEP diagram of the molecular structure of [(L^5)Zn (**5b'**). Thermal ellipsoids are drawn at the 30% probability level. Selected bond lengths (Å) and angle (°): Zn1−O2 1.885(3), Zn1−O1 1.923(3), Zn1−N1 2.023(3), Zn1−N3 2.062(4), O1−Zn1−N1 94.0(14), O1−Zn1−N3 119.0(14), N1−Zn1−N3 104.8(14), O1−Zn1−O2 125.9(13), N1−Zn1−O2 117.8(13), N3−Zn1−O2 95.1(14).

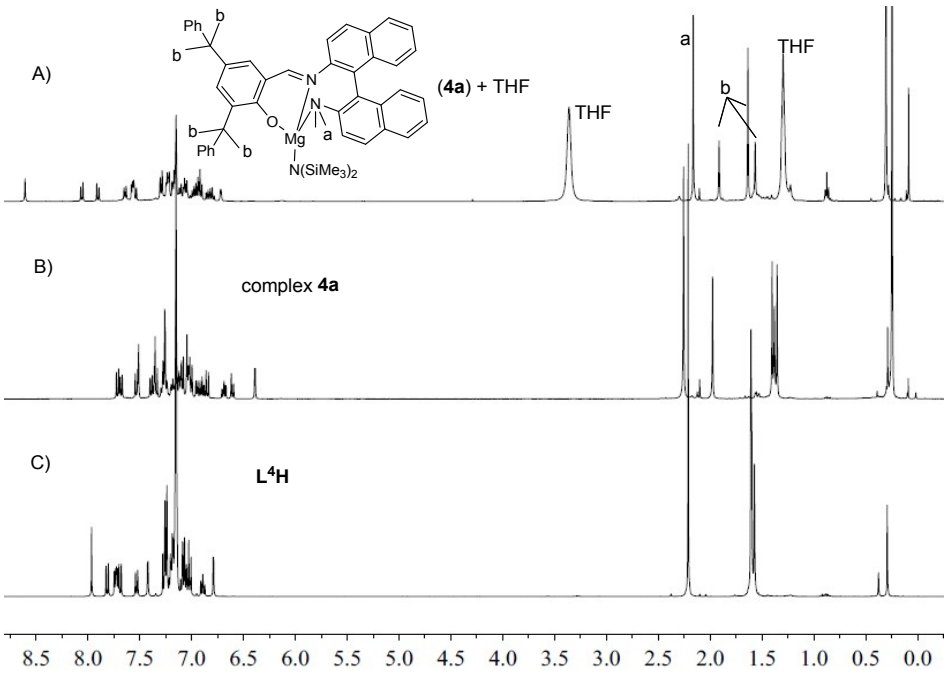

Figure S2. A) ^{1}H NMR spectrum of magnesium complex **4a** in C_6D_6, one tiny drop of THF was added; B) ^{1}H NMR spectrum of complex **4a** in C_6D_6; C) ^{1}H NMR spectrum of free ligand **L^{4}H** in C_6D_6 (400 MHz).

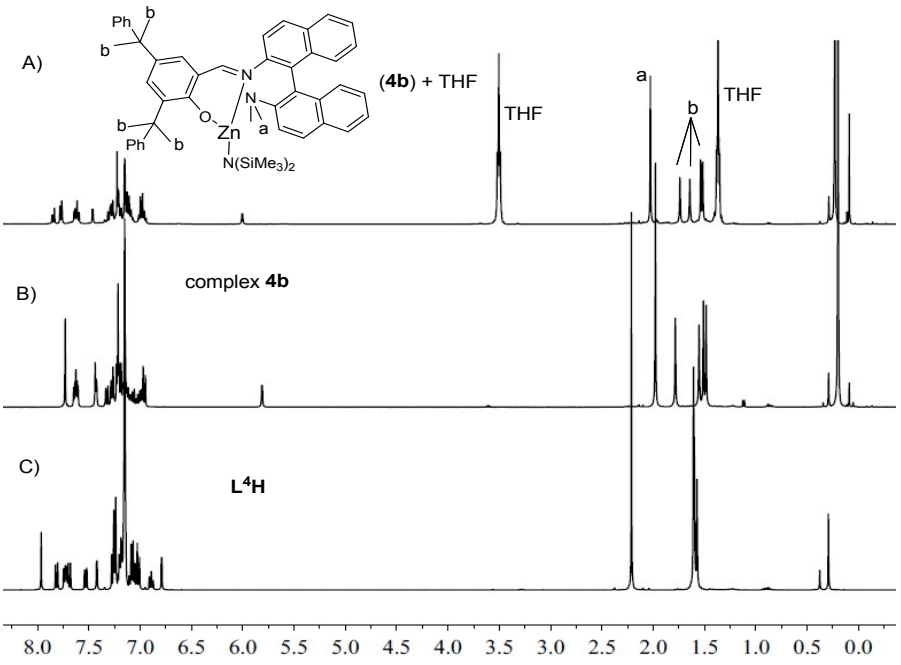

Figure S3. A) ^{1}H NMR spectrum of zinc complex **4b** in C_6D_6, one tiny drop of THF was added; B) ^{1}H NMR spectrum of complex **4b** in C_6D_6; C) ^{1}H NMR spectrum of free ligand **L^{4}H** in C_6D_6 (400 MHz).

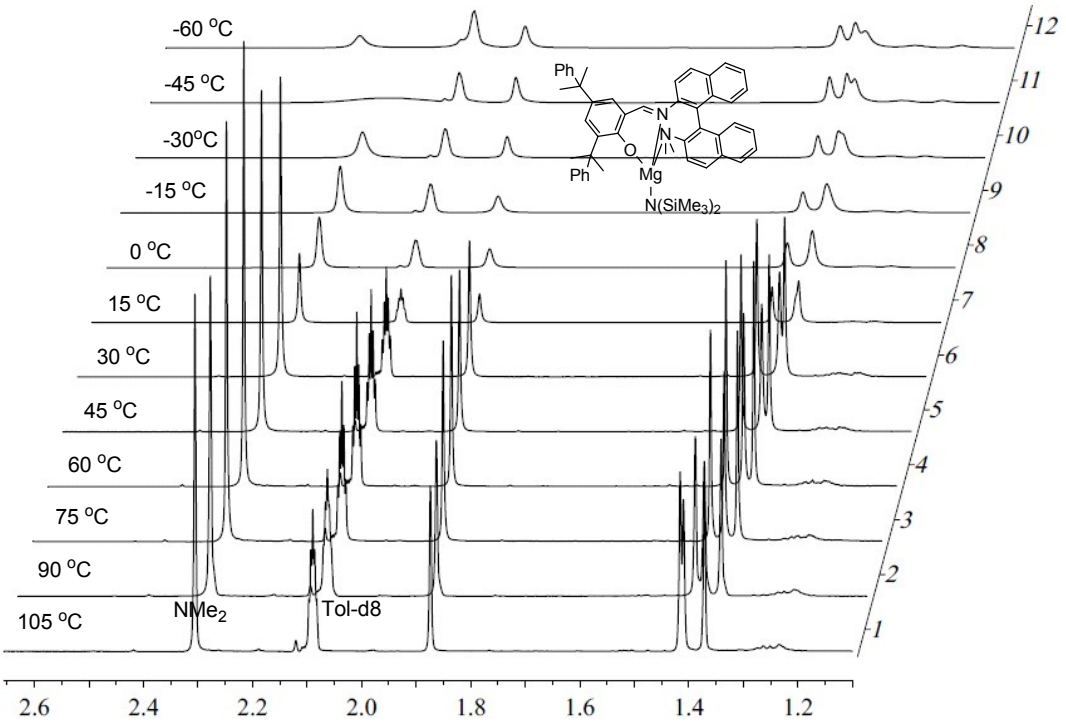

Figure S4. The variable temperature ^{1}H NMR spectra of complex **4a** (toluene-d_8, 400 MHz; partial signals are shown).

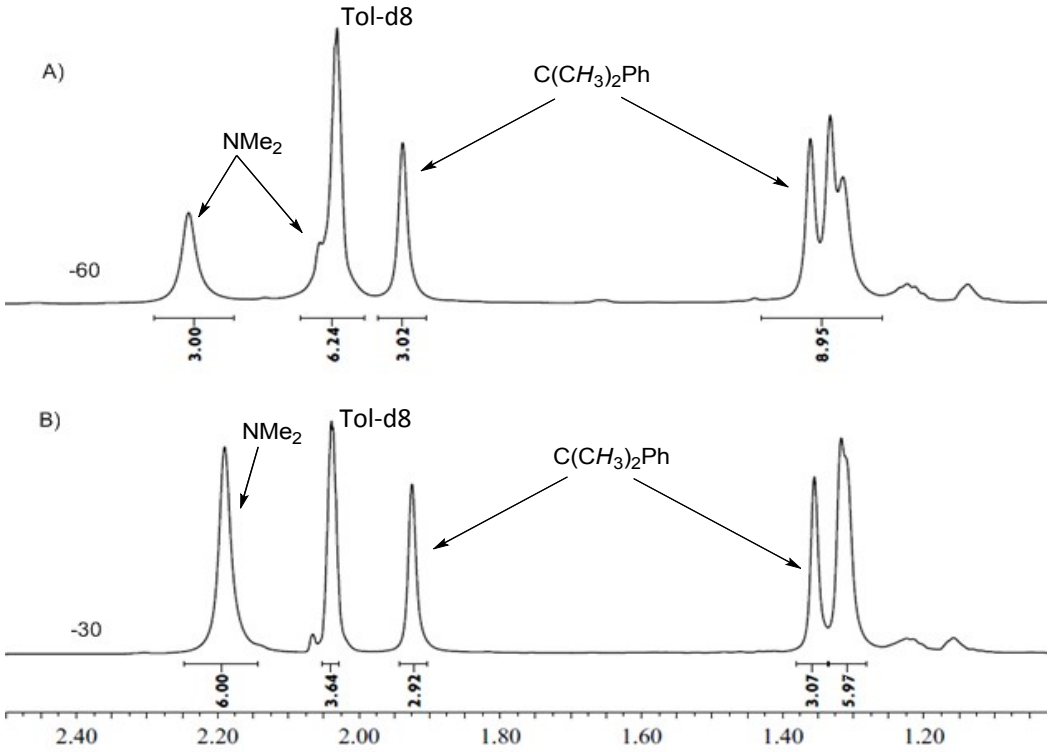

Figure S5. The variable temperature ^{1}H NMR spectra of complex **4a** at –60 °C and –30 °C (toluene-d_8, 400 MHz; partial signals are shown).

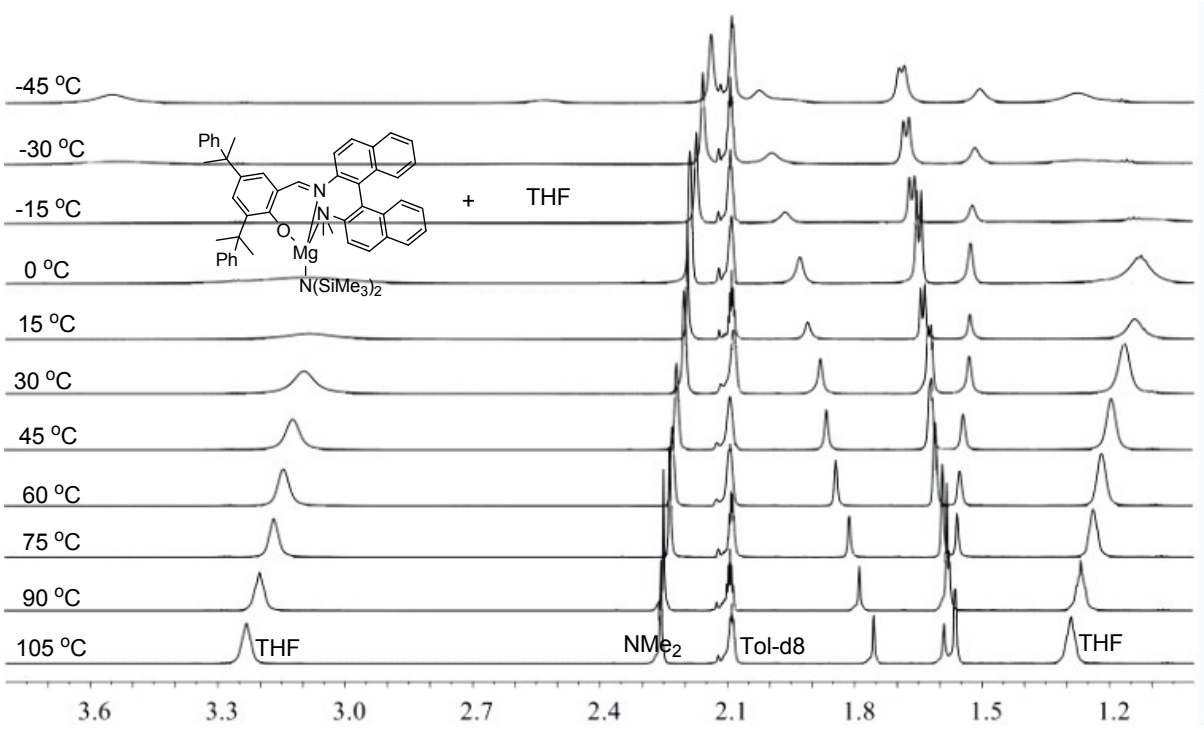

Figure S6. The variable temperature ^{1}H NMR spectra of complex **4a** with 2 equiv. of THF (toluene-d_8, 400 MHz; partial signals are shown).

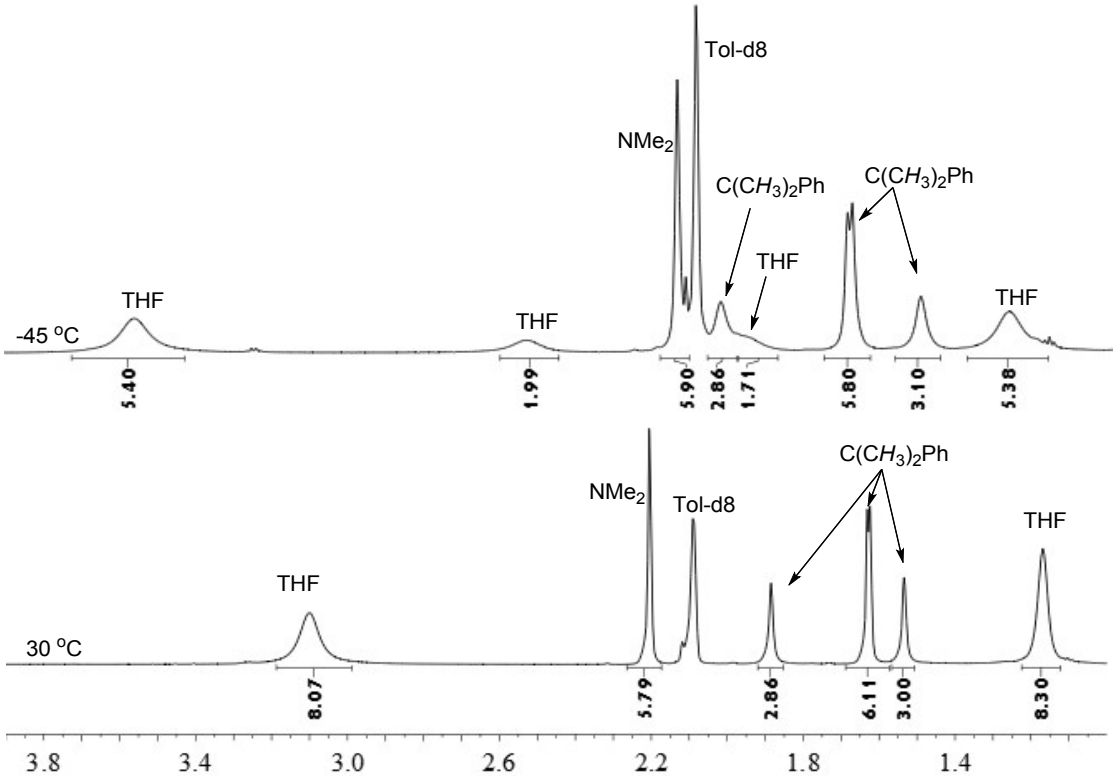

Figure S7. The variable temperature ^{1}H NMR spectra of complex **4a** with 2 equiv of THF at –45 °C and 30 °C (toluene-d_8, 400 MHz; partial signals are shown).

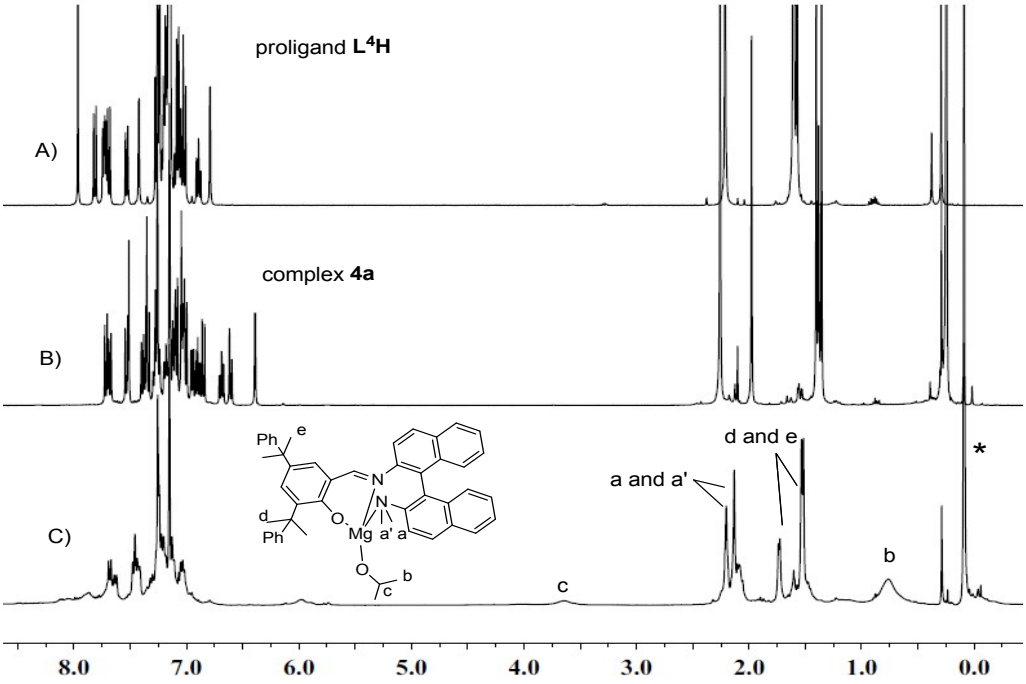

Figure S8. A) ^{1}H NMR spectrum of free ligand **L^{4}H** in C_6D_6; B) ^{1}H NMR spectrum of complex **4a** in C_6D_6; C) ^{1}H NMR spectrum of the reaction mixture between complex **4a** and one equiv. of 2-propanol (C_6D_6, 400 MHz, *, $HN(SiMe_3)_2$).

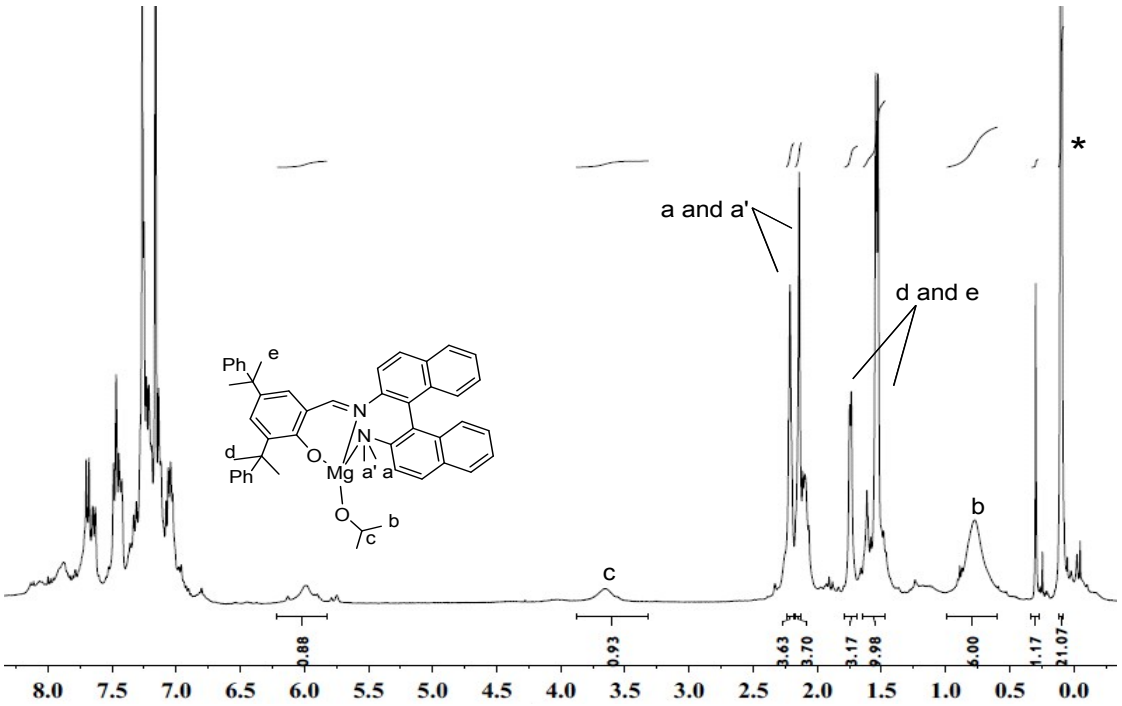

Figure S9. ^{1}H NMR spectrum of the reaction mixture between complex **4a** and one equiv. of 2-propanol (C_6D_6, 400 MHz; *, $HN(SiMe_3)_2$).

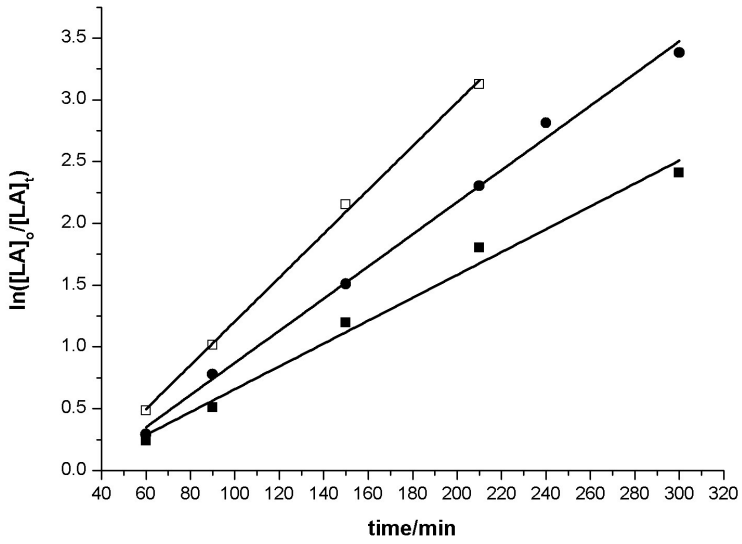

Figure S10. Kinetics of *rac*-LA polymerization initiated by complexes **4a**-**6a**/^{i}PrOH in toluene with [*rac*-LA]$_0$ = 1 mol/L, 25 °C. □: [*rac*-LA]$_0$/[**4a**]$_0$/ [^{i}PrOH]$_0$ = 200/1/1, k_{app} = 0.018 min^{-1}; ●: [*rac*-LA]$_0$/[**5a**]$_0$/[^{i}PrOH]$_0$ = 200/1/1, k_{app} = 0.013 min^{-1}; ■:[*rac*-LA]$_0$/[**6a**]$_0$/[^{i}PrOH]$_0$ = 200/1/1, k_{app} = 0.0093 min^{-1}.

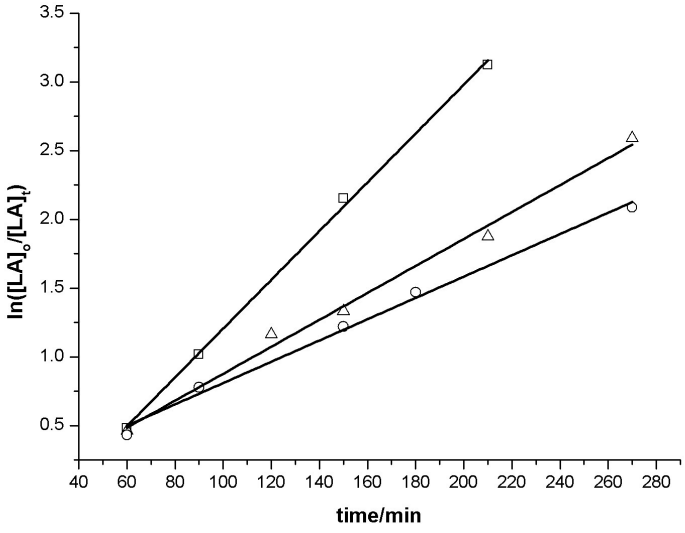

Figure S11. Kinetics of *rac*-LA polymerization initiated by [**4a**]/[^{i}PrOH] in toluene at 25 °C with [LA] = 1 mol·L^{-1} (□: [*rac*-LA]$_0$/[**4a**]/[^{i}PrOH] = 200/1/1, k_{app} = 0.0177 min^{-1}; ∆: [*rac*-LA]$_0$/[**4a**]/[^{i}PrOH] = 400/1/1, k_{app} =0.00959 min^{-1}; ○: [*rac*- LA]$_0$/[**4a**]/[^{i}PrOH] = 500/1/1, k_{app} = 0.0078 min^{-1}).

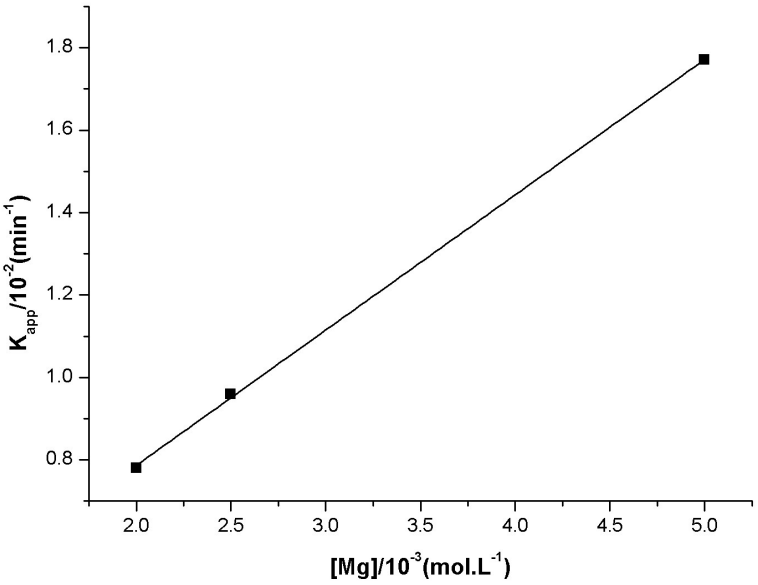

Figure S12. Plot of k_{app} *versus* the concentration of **4a** for *rac*-LA polymerization at 25 °C in toluene by **4a**/2-propanol ([*rac*-LA] = 1 mol·L^{-1}, k_p = 3.52 L·mol^{-1}·min^{-1}).

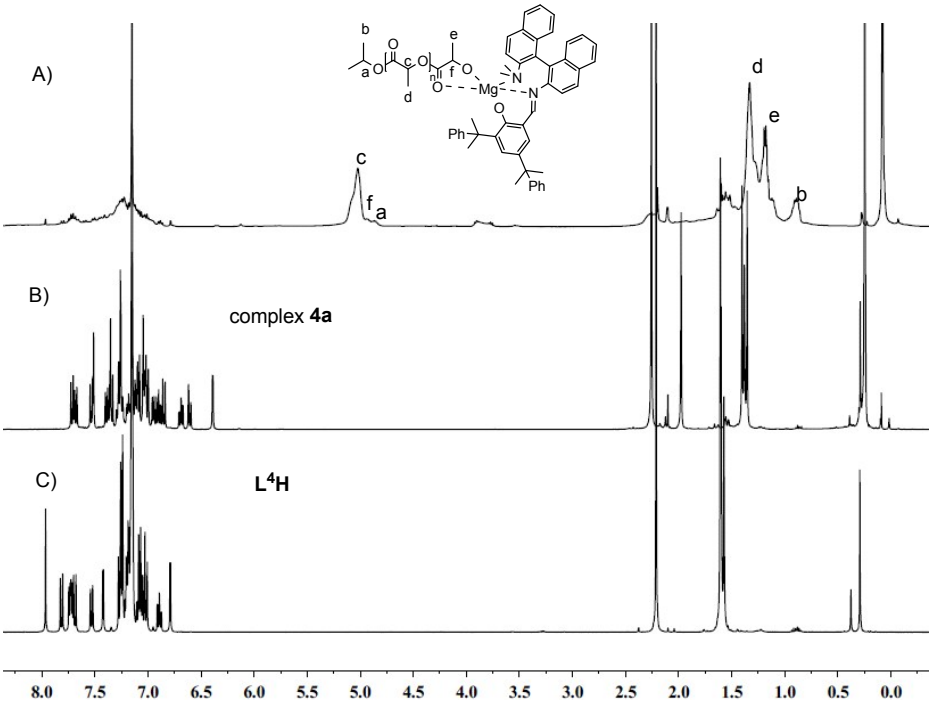

Figure S13. A) ^{1}H NMR spectrum of active *rac*-lactide oligomer obtained by complex **4a**/ ^{i}PrOH system ([*rac*-LA]$_0$: [Mg]$_0$: [^{i}PrOH]$_0$ = 20:1:1, at 25 ºC); B) ^{1}H NMR spectrum of complex **4a**; C) ^{1}H NMR spectrum of free ligand **L^{4}H** (C_6D_6, 400 MHz).

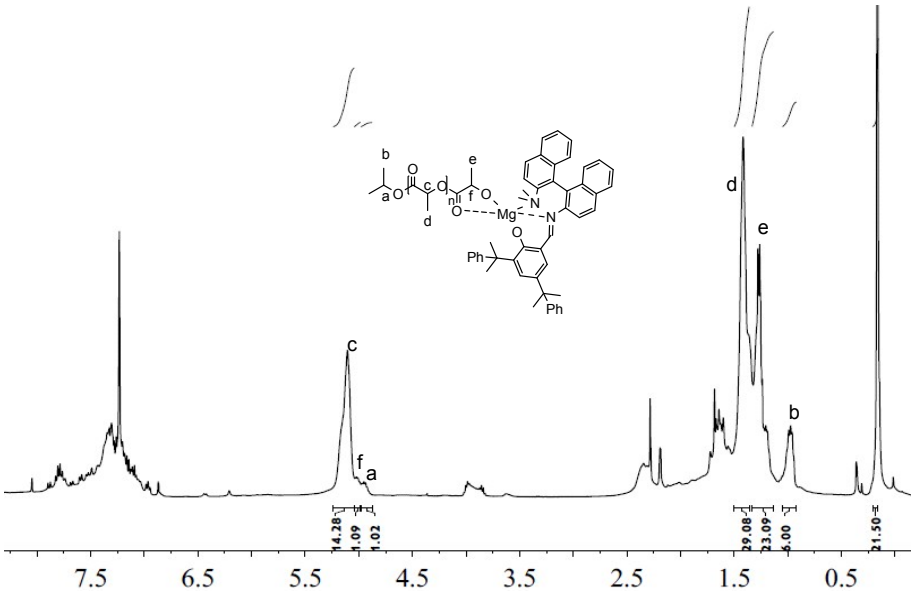

Figure S14. ^{1}H NMR spectrum of active *rac*-lactide oligomer obtained by complex **4a**/ ^{i}PrOH system (C_6D_6, 400 MHz; [*rac*-LA]$_0$: [Mg]$_0$: [^{i}PrOH]$_0$ = 20:1:1, at 25 ºC).

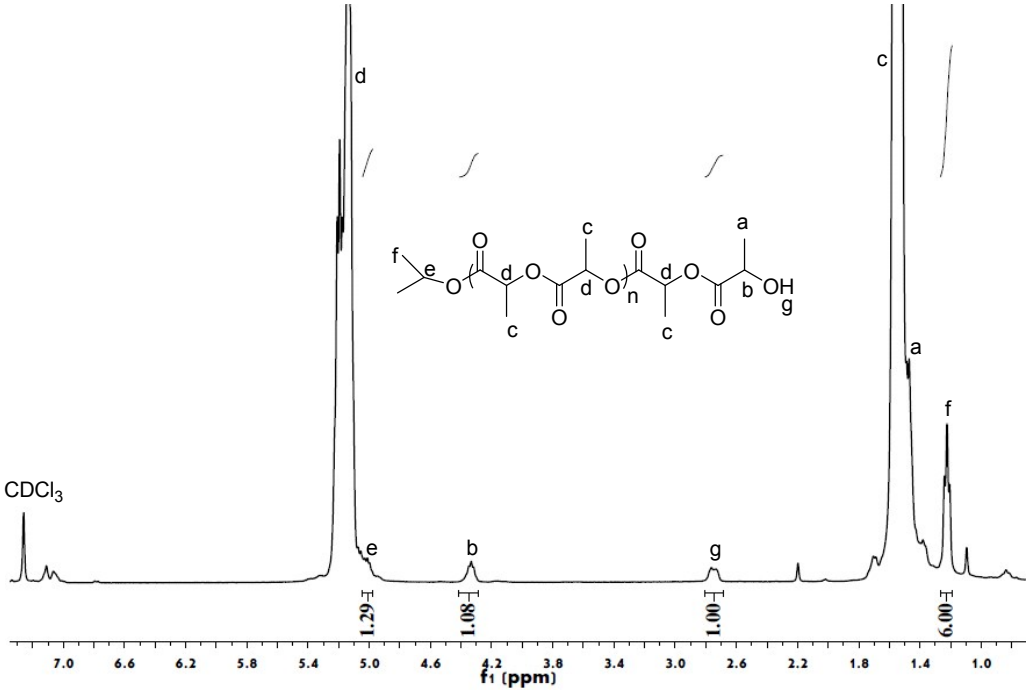

Figure S15. ^{1}H NMR spectrum of typical polymer sample obtained by **4a**/isopropanol system with [*rac*-LA]/[**4a**]/[^{i}PrOH] = 20 : 1 : 1 at 25 °C in THF.

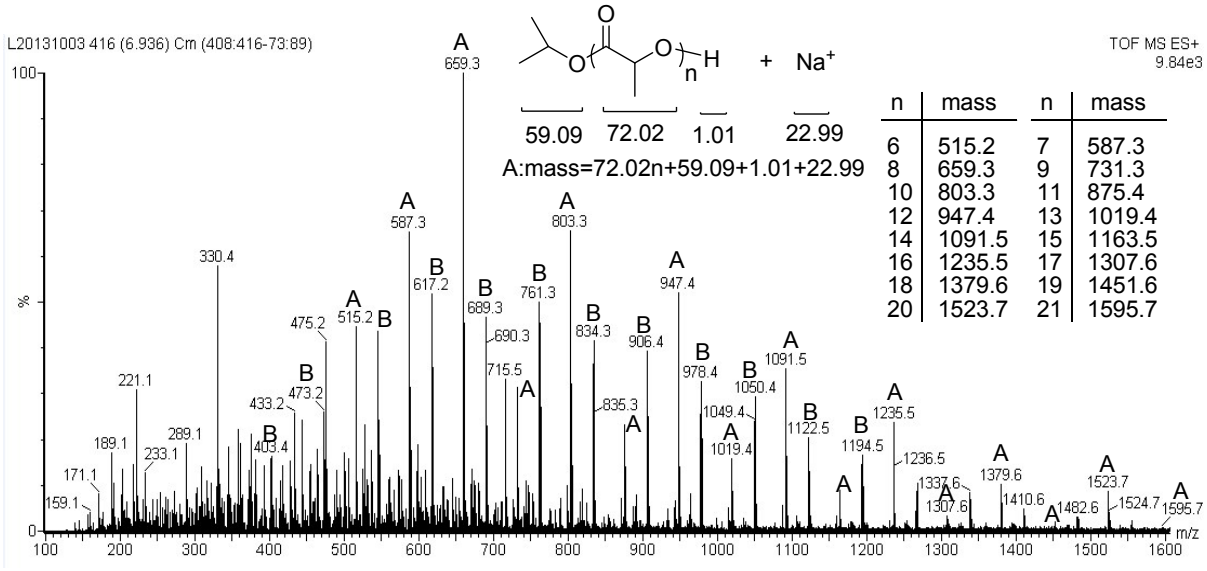

Figure S16. ESI-TOF mass spectrum of the *rac*-LA oligomer obtained with **4a** ([*rac*-LA]$_0$: [**4a**]$_0$: [^{i}PrOH]$_0$ = 20:1:1, in THF; **B:** cyclic oligomers + K^+ + 2).

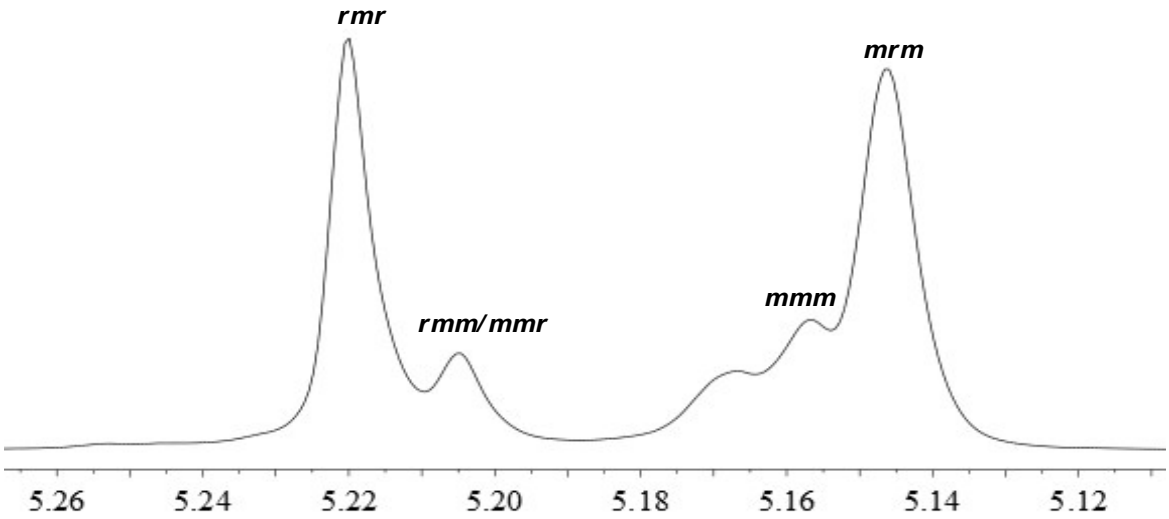

Figure S17. Homonuclear decoupled ^{1}H NMR spectrum of PLA produced from *rac*-lactide using **4b** as the initiator. ([*rac*-LA]$_0$ = 1 M, [**4b**] = [^{i}PrOH] = 0.5 mM, 97% monomer conv., in THF, 25 ^{o}C, P_r = 0.83).

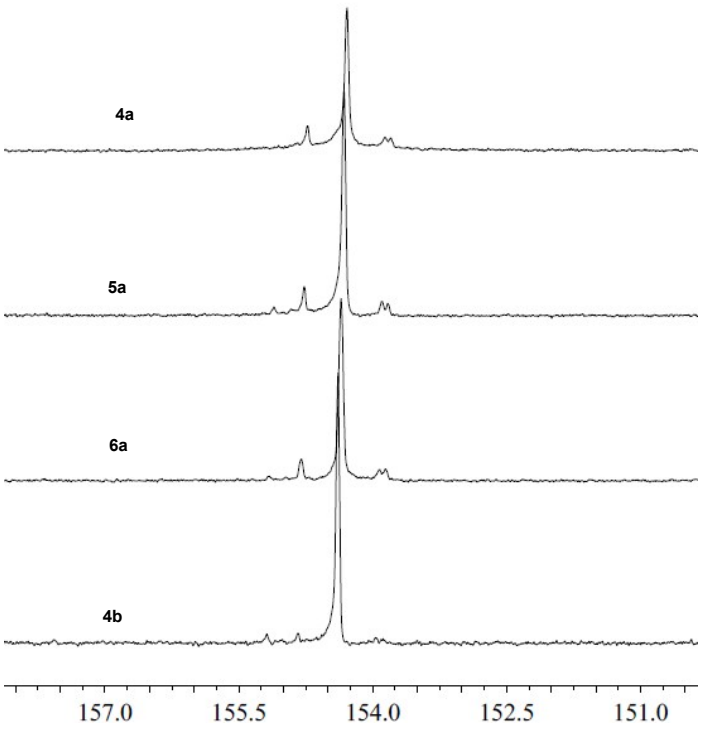

Figure S18. Details of the carbonyl region of the $^{13}C\{^{1}H\}$ NMR spectra (100 MHz, $CDCl_3$, 25 °C) of poly(α-MeTMC)s: **4a** (Table 3, Run 1) (X_{reg} = ca. 0.78), **5a** (Table 3, Run 2) (X_{reg} = ca. 0.83), **6a** (Table 3, Run 3) (X_{reg} = ca. 0.82), **4b** (Table 3, run 4) (X_{reg} = ca. 0.98).

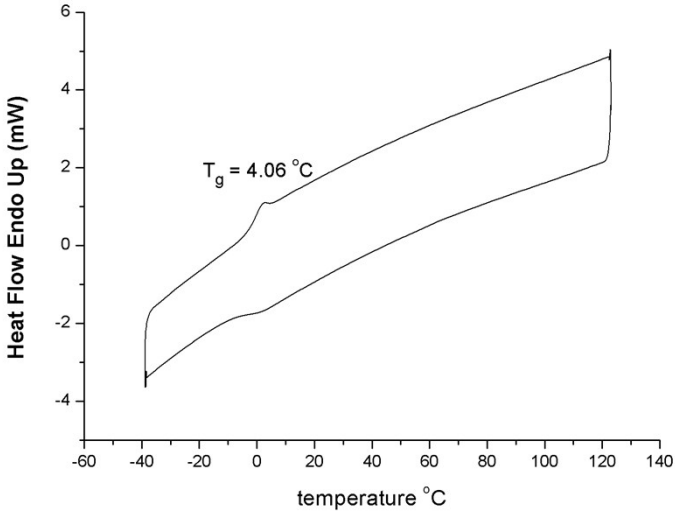

Figure S19. The DSC curves of poly(α-MeTMC) produced from α-MeTMC using **4b** as the initiator ([α-MeTMC]$_0$ = 1 M, [**4b**] = 0.5 mM, 90% monomer conv., in toluene, 25 °C, T_g= 4.06 °C).